Numerical analysis of energy recovery system for turbocharged internal combustion engines via a parallel compounding turbine

Numerical analysis of energy recovery system for turbocharged internal combustion engines via a parallel compounding turbine

Stefano Frigo, *Marco* Francesconi, *Luca* Sani and *Marco* Antonelli*

University of Pisa, D.E.S.Te.C. Departimento, 26122 Pisa, Italy

Abstract. Increasing energy efficiency requirements mandatory ask for optimizing energy utilization in many devices, which include internal combustion engines. One of the most investigated subjects is the energy recovery from the exhaust, such as turbo-compound systems, which usually consist in a secondary turbine located afterward the turbocharger. Here an alternative arrangement is proposed and analysed via a numerical model. The recovery turbine works in parallel to the main turbine and uses the gasses which would be otherwise wasted through the waste-gate valve, once the set-point boost pressure is reached. The reference case analysed is a 12.4L turbocharged diesel engine, commonly used in marine, road and light railroad applications, with a nominal power of 380kW. The results showed that an overall 8% of power can be gained, without nor increasing the fuel mass flow rate, neither requiring significant modifications to the baseline engine. Moreover, in the case of the recovery system failure, the operation of the engine is not affected, thus resulting in no engine availability reduction. This work also shows a feasible way to convert the mechanical energy delivered by the recovery turbine into electrical energy, by making use of a high-speed electrical generator.

1 Introduction

Fuel-saving in internal combustion engines is a promising aspect of reducing pollutant emissions and increasing autonomy [1-3].

Several possibilities, such as Rankine Organic Cycle (ORC), Thermo-Electric Generator (TEG) and turbo compounding, allow recovering waste energy from the energy [1,4,5].

Despite it was introduced more than 100 years ago, turbo compounding remains an attractive solution that has been proposed in the last decades to improve the energy efficiency of commercial engines [6–8]. Its central principle consists of a turbine that recovers the energy of the wasted gas discharged from the cylinders. The recovered energy is then available to drive the engine crankshaft or a compressor to boost the inlet air pressure.

Over several years, the development of turbo compound led to several configurations which differ in the shaft arrangement or in the use of one or two stages for the expansion process [7].

* Corresponding author: marco.antonelli@unipi.it

Another aspect that characterizes a turbo compound system is the possibility of converting the recovered energy into electrical energy as proposed by the Electrical Turbo Compound (ETC) technology [9-13]. It consists on an electrical machine, connected to the turbocharger, able to recover the excess power furnished by the turbine (generator mode) or, during acceleration, to accelerate the turbo hence reducing the turbo lag (motor mode). In the last years, this aspect has become attractive because it fits the necessities of the recent vehicles that consume a significant amount of electrical energy owing to the wide use of several auxiliary electrical systems [14]. The advantages of the ETC technology are the flexibility, cheaper implementation that does not require a gearbox in the integration with the crankshaft [10] and compactness, as shown by Hopmann and Arsie [9][11].

Some studies demonstrated the convenience of ETC technology by showing an increase in the fuel efficiency between 3-5%, which can reach a peak of 10% under nominal operating conditions of the engine [9][15] .

Besides, Frigo et al. evaluated by a numerical code the integration of the ETC system into a twin-cylinder small SI engine with a displacement of 900 cm^3 [16]. They claimed that the overall efficiency of the engine with ETC improved when it provided a variable power output. In a subsequent work [17], Eggimann et al. carefully evaluated the integration of the ETC concept in a full vehicle following the WLTC driving cycle, evidencing the importance of sizing the ETC unit for the average power required by the vehicle and not for the maximum that can be obtained from the engine.

However, the main drawback of the turbo compound systems, also affecting ETC technology, is that when the exhaust back pressure is higher, it increases the rotating speed of the turbine. The consequence is that the compressor causes an unacceptable pressure increase that may damage the engine.

In commercial engines, this problem is solved introducing a wastegate valve which allows a part of the exhaust gases to bypass the turbine, thus limiting the power transferred to the compressor, or with the adoption of a variable geometry turbine (VGT). However, the wastegate dissipates part of exhaust gases enthalpy.

To avoid this, Zhuge et al. proposed to recover this energy by another turbine to drive an electric generator (turbo-generator) [14] as suggested by the ETC technology. Their work numerically investigated an engine in which a turbo-generator was parallel with the turbocharger. The analysis considered both a fixed and variable geometry for the turbine in the turbo-generator. The results suggested an improvement in the fuel efficiency up to 4.7% and that the use of a variable turbine geometry was significant in operating conditions with high load.

This paper shows the first results of a numerical investigation dedicated to evaluating the betterments generated by the application of a recovery turbine added in parallel to the original turbocharger of the engine. As a case study, a 12.4L turbocharged diesel engine with a nominal power of 380kW was considered because it is used in marine, road and light railroad applications.

The investigation led to establish the relationship between the mass flow rate released by the WG valve in absence of a recovery system and the sizing of the recovery turbine, as well as the effectively recoverable mechanical power. The study considered recovery turbines derived from commercial turbochargers, even though a certain optimization can improve the results by fitting the turbine shape to the task of recovering the waste energy.

2 Method

This recovery system was analysed by observing the power delivered by the engine and by the added recovery turbine. Due to the preliminary nature of the study, only a numerical model was developed, by adopting the simulation environment AMESim. The numerical model simulates a typical diesel engine for truck, maritime and light railroad applications,

with 6 in-line cylinders, turbocharged and aftercooled (figure 1), whose main features are summarized in table 1.

Table 1. Main engine features

Feature	Value	Unit
Bore	126	mm
Stroke	166	mm
n. of cylinders	6	--
Total displacement	12.4	L
Rated power	382	kW
Maximum speed	2000	Rpm
Rated torque	2360	Nm
Max torque speed	1100-1400	rpm

The engine was simulated thorough a lumped parameter model, which accounted for the fluid dynamic and heat transfer phenomena in the cylinders, inlet/exhaust manifolds, turbocharger and intercooler. The model also accounted for mechanical friction, by using a simple quadratic, algebraic function of the rotating speed. Combustion was modelled with the approach of Chmela et Al. [18, 19]. No changes were made to the default combustion coefficients of the model. Fuel evaporation time was also accounted as a function of the in-cylinder temperature. Fresh charge inflow and exhaust gasses outflow were regulated by the opening and closure of intake and exhaust valves, which were modelled as variable area orifices. Compressor and turbine were simulated by means of their non-dimensional maps, reporting the corrected flow rate and efficiency as a function of pressure ratio and corrected rotating speed.

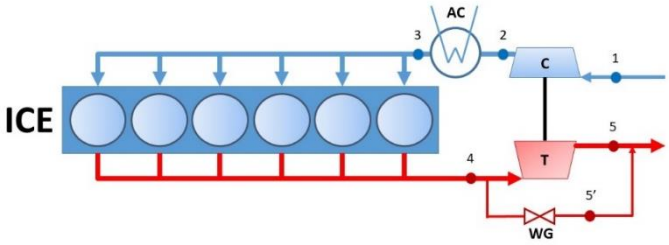

Figure 1. Scheme of a turbocharged, aftercooled internal combustion engine. ICE – Internal Combustion Engine, AC – Aftercooler, C – Compressor, T – Turbine, WG – waste-gate valve

This numerical model was calibrated in order to reproduce the behaviour of the engine reported in readily available datasets. After calibration of the mechanical injection duration and advance, engine torque and specific fuel consumption were predicted with an incertitude of 2% (figures 2 and 3). At full load, the equivalence ratio φ was between 0.53 and 0.82, as currently happens in high-performance diesel engines, with a boost pressure limited to 2.4 absolute bar (figure 4) by opening the waste-gate (WG) valve.

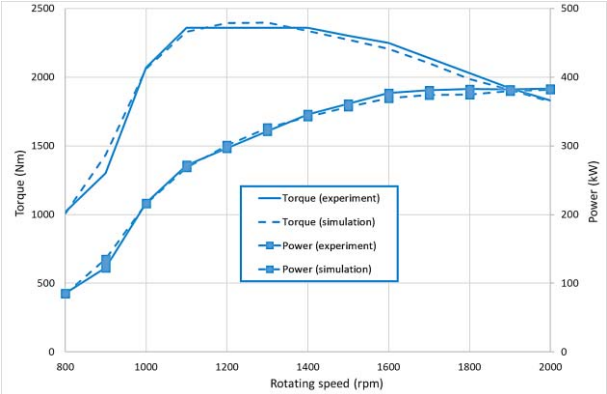

Figure 2. Experimental vs. simulated torque as a function of the rotating speed, full load condition

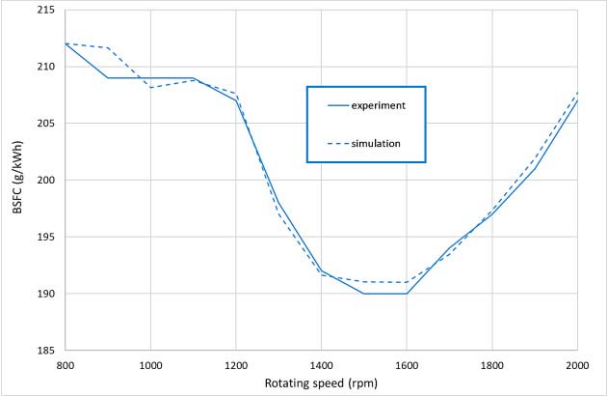

Figure 3. Experimental vs. simulated BSFC as a function of the rotating speed, full load condition

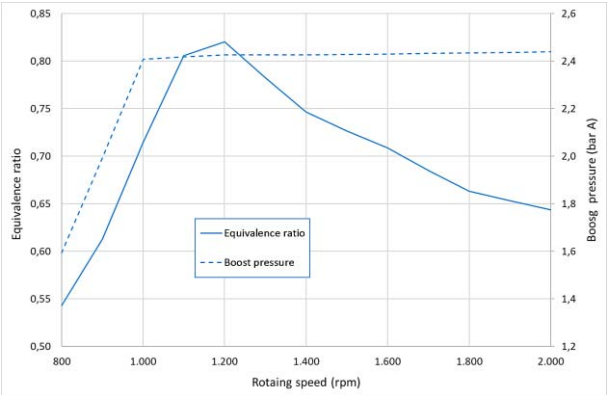

Figure 4. Equivalence ratio and boost pressure as a function of the rotating speed, full load condition

1.1 Application of the recovery turbine

As stated in the previous lines, the supercharging pressure was controlled through the opening of the WG valve, which is an inherently dissipative mean. The wasted energy P_w was calculated as the power that could be generated by isentropically expanding the mass flow passed by the valve with the pressure ratio between the exhaust manifold and the ambient air. Thus, it was calculated by multiplying the mass flow rate through the WG valve by the specific energy content:

$$P_w = \dot{m} \cdot \frac{kRT_4}{k-1} \cdot \left[\left(\frac{p_4}{p_5} \right)^{\frac{k-1}{k}} - 1 \right]$$

The wasted power was zero at 1000 rpm, since there was no excess energy in the exhaust. Beyond 1100 rpm, exhaust mass flow rate exceeded the amount necessary to the turbine and WG valve started to open. Power dissipation thus increased with rpm (figure 5), up to a maximum of about 67.5 kW at the maximum speed of the engine (2000 rpm). This also means that, if fully recovered, gasses exhausted by the WG valve may add 17.7% of power to the engine.

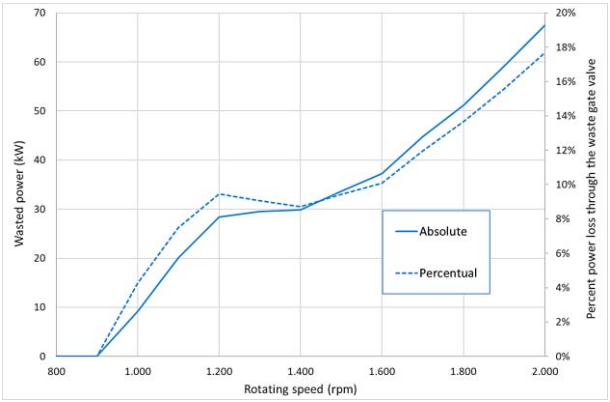

Figure 5. Power loss through the WG valve as a function of rotating speed

A secondary turbine was added in parallel to the turbocharger turbine (figure 6), so that it could use the gasses otherwise ejected by the WG valve. A valve (CV), controlled by the intake manifold pressure, regulates the gas flow through the recovery turbine, in order to keep constant the boost pressure. The original WG valve, however, was kept in place, with the aim of controlling the manifold pressure in the case that the auxiliary turbine regulation valve was already fully open. The two valves were operated in way that the WG valve started to open only once the control valve was already fully open.

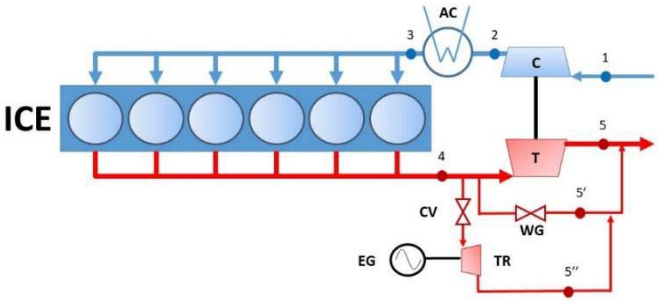

Figure 6. Scheme of the engine after application of the recovery turbine. CV – Control valve, EG – Electric generator, TR – Recovery turbine

As for the implementation of the recovery system, in this first work the authors have hypothesized to use a commercial turbocharger, converted into a recovery turbine by replacing the compressor with a high-frequency electric generator. The turbine was selected on the basis of the corrected mass flow rate available $\dot{m}_c$, defined as:

$$\dot{m}_c = \dot{m}_4 \frac{\sqrt{T_4}}{p_4}$$

The corrected mass flow rate available (figure 7) in the analysed application ranged from zero at idle to 13.3 g/s $K^{1/2}$/kPa at the speed of maximum engine torque and 23.6 g/s $K^{1/2}$/kPa at the speed of maximum power.

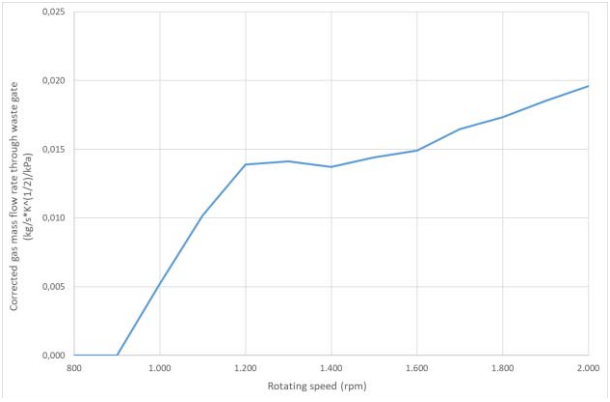

Figure 7. Corrected mass flow rate through the WG valve

It is necessary to pay attention to the selection of the turbine used for the energy recovery: if the machine is small, it will efficiently recover the exhaust energy at low engine speed, but it will not be able to manage the excess mass flow rate at high rpm. Therefore, it will result in a poor recovery capability when the engine delivers its maximum power. Conversely, a larger turbine allows a more complete energy recovery at high engine rpm, but has a lower recovery capability at low engine speed. Therefore, it is worthy to choose the right machine by considering the typical mission profile of the engine, as evidenced in other studies [16].

In the considered case, several turbine models, all from Garrett, were selected for the investigation, based on their swallowing capacity in chocked conditions (table 2). The smallest turbine was the GT2052 and the largest was the G25-550 trim 72. Their chocked mass flow rate are 14.2 and 25.0 g/s $K^{1/2}$/kPa, respectively, which corresponded to the corrected mass flow rates exhausted through the WG at maximum torque and maximum engine power regimes. A medium size turbine was also tested, model GT2859r, with a chocked corrected mass flow rate of 19.1 g/s $K^{1/2}$/kPa.

Table 2. Turbochargers used as recovery turbines

Model	Chocked corrected mass flow rate (g/s $K^{1/2}$/kPa)	Max efficiency (%)
GT2052	12.8	72%
GT2859r	19.1	75%
G25-550 trim 72	25.0	74%

3 Results and discussion

The behaviour of the system was evaluated by observing the additional power delivered by the recovery turbine, since the application of this system does not alter the performance of the engine at all. Power delivered by the engine alone, here not reported for brevity sake, was in effects identical to the baseline case. The turbine additional power was reported as a percent of the net engine power, with no added recovery system.

3.1 Application of the recovery turbine

In general terms, the recovery turbine delivered additional power increasingly with the rotating speed (figure 9), since the faster runs the engine, the larger is the exhaust gas excess mass flow rate.

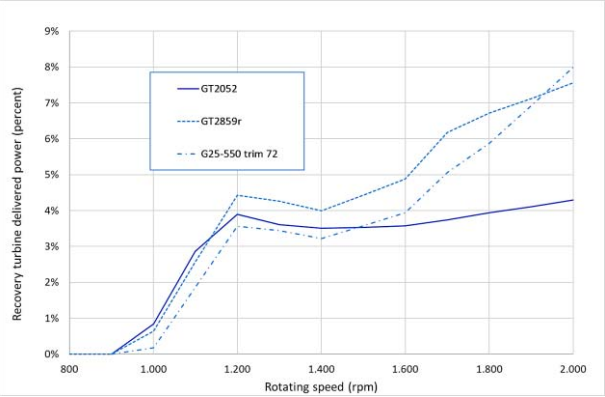

Figure 8. Additional percent power delivered by the recovery turbine

Below 1000 rpm, WG valve was closed and no additional power could be delivered. After then, additional power increased up to 5.4 – 8.7% at the maximum engine speed. As expected, the application of the smallest turbine gave the better improvement at low engine speed (up to 1100 rpm). This small turbine added very small power for two reasons:

- Its throat area is so small that the WG valve of the engine turbocharger started to open at 1200 rpm, thus dissipating a lot of energy since medium rpm;
- The efficiency of this turbine is reduced respect to the others, so it did not recover the exhaust energy as efficiently as the others.

The largest turbine provided the best improvement only at maximum engine speed, since its performance was poorer than all the others below 1500 rpm. Its throat area is in facts quite large, compelling the control valve to be kept more closed than in the other cases at all the engine regimes.

3.2 Influence of the turbine size

The best performance over the most part of the engine operating range was achieved by using the medium size turbine, which gave the better power improvement from 1200 up to 1900 rpm. Over 1800 rpm it was necessary to open the WG valve, since its throat area was too small to fully accommodate the whole exhaust mass flow rate.

Due to the different throat area of the investigated turbines, the control valve underwent different opening grades as a function of the engine rotating speed (figure 10). Using GT2052 as a recovery turbine led to the full valve open at 1200 rpm, GT2859r at 1800 rpm, while in the case of the G25-550 trim 72 the valve was never completely open.

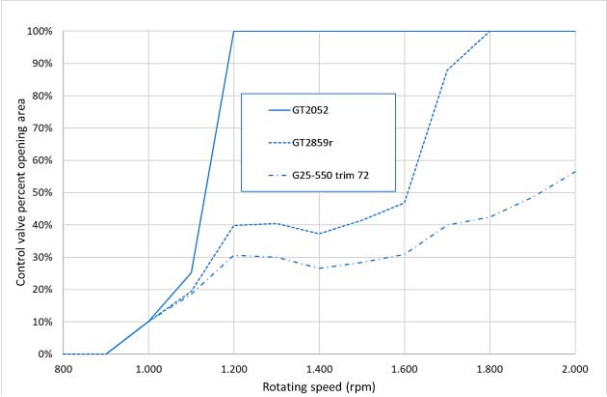

Figure 9. Control valve percent aperture as a function of rotating speed

The use of a small turbine allowed the reduction of the lamination loss across the control valve (figure 11), as witnessed by the small pressure difference between the exhaust manifold and the recovery turbine inlet. On the other hand, a relevant portion of the excess mass flow rate was exhausted through the WG valve (up to 13% of the engine exhaust mass flow rate, figure 12). Using larger turbines, in one hand led to larger lamination losses through the control valve in most part of the engine rotating speed range, in the other it reduced the mass flow rate exhausted through the WG valve. The largest turbine allowed the recovery of the entire mass flow rate, by keeping the WG valve always closed, but at the expense of a larger pressure dissipation through the control valve.

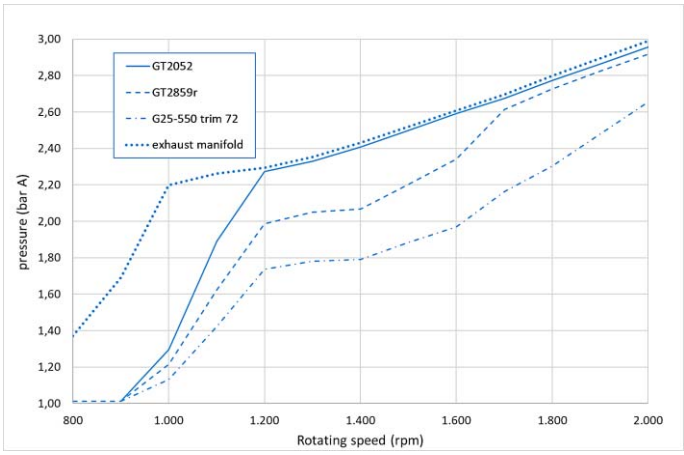

Figure 10. Pressure comparison between the exhaust manifold and the recovery turbine inlet as a function of rotating speed

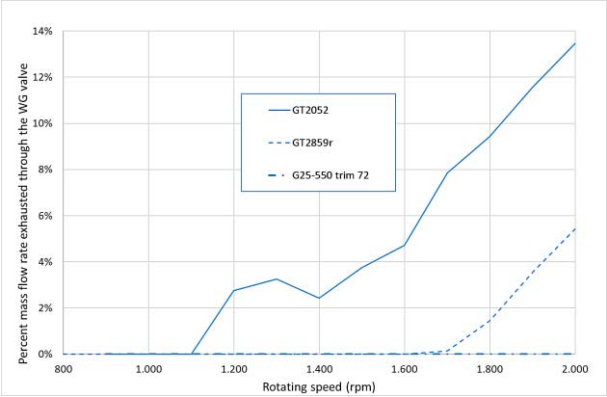

Figure 11. Percent mass flow rate through WG valve as a function of rotating speed

3.3 Engine performance improvement

The application of this recovery system led to the reduction in the specific fuel consumption (figure 13), which was more significant at high engine speed, but was not negligible even at very low engine speed (1000 rpm).

Even though the smaller turbine showed a better recovery capability at low rpm, the difference with a larger turbine was practically insignificant up to 1300 rpm. Beyond this speed, the medium size turbine exhibited a much more evident power recovery. The largest turbine, instead, showed the worst general behaviour. Only at the maximum speed, it overcame the performance of the medium size turbine.

These results indicate that the recovery system shows the best performance when the recovery turbine corrected mass flow rate is in between the maximum torque and the maximum power available corrected mass flow rate. With a recovery turbine sized in this way, the engine minimum BSFC rpm slightly increased (from 1500-1600 rpm to 1700) and the specific consumption decreased from 191 to 182 g/kWh (-4.9%). At the engine maximum speed, BSFC decreased from 208 to 192 g/kWh (-7.7%).

It is worthy to point out that the recovery system also allows the BSFC curve to be flatter. In facts, the baseline engine BSFC increased from the best efficiency point to the maximum power condition by 8.9%, while the recovery system limited the BSFC increase to only 5.2%.

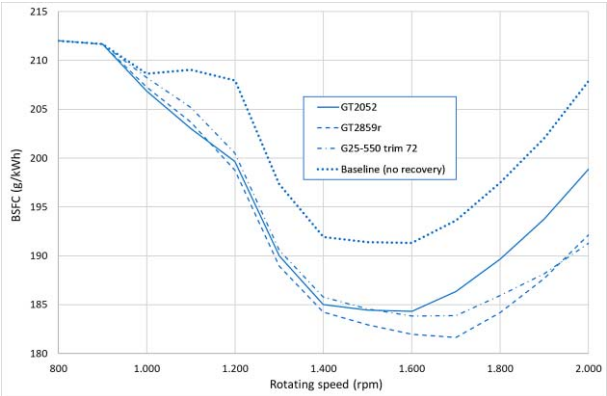

Figure 12. BSFC vs. rotating speed for different recovery turbine models

It is worthy to point out that these results were obtained by means of turbines derived from commercial turbochargers, whose efficiency never exceed 72-73% along the investigated cases. If an optimization process on improving the recovery performance of the turbine would take place at the expense, for instance, of the transient behaviour, which is not a determining factor in this application, even better results could be obtained.

3.3 High-speed electric generator

The recovery turbine rotates at the same speed of a conventional turbocharger, i.e. from 50000 to 150000 rpm, or even more. One method for summing the power delivered by the turbine to the power delivered by the engine is the accommodate a mechanical gear to reduce the speed of the shaft, but there are some concerns in developing high-speed gears and in the mechanical losses entailed by the mechanism. An alternative method is the use of a high-speed generator, especially if the internal combustion engine driving an alternator, such as in prime movers, railway application or on-board marine generators.

Compared with low-speed and moderate-speed conventional electrical machines, high-speed electrical machines (HSM) offer advantages such as high-power density, small size, and light weight [20]. With the evolution in the field of power electronics converters, the problems of high frequency supplies, required for high-speed operation, is no longer a restriction.

The choice of machine topology depends on many factors such as: environment (temperature, volume size), specifications (torque, speed, acceleration, etc.) and cost. In the field of HSM, brushless Permanent Magnet motors appear to be the most widely used solution. The design of an HSM needs to consider many aspects: the electromagnetic one, due to the high operating frequencies, the structural one, due to the critical speeds, and the thermal one, because the dimensions are small.

The machine design starts with analytical design calculations based on the requirements (Table 2) established along the previously presented fluid dynamic analysis.

Table 2 Requirements of the high-speed generator

Rated Power (P_N)	20 kW
Rated speed (n)	160 krpm
Supply frequency	< 3000 Hz
Efficiency	> 0.95

An electrical machine with a high number of poles is not possible, on account of the high speed. Hence, only a design with two or four poles is possible. To stay within the supply frequency requirement a model with two poles was selected.

Since rare-earth permanent magnets of the rotor are brittle, they are not mechanically strong enough to bear the centrifugal force resulted from the high rotational speed. Therefore, it is needed to carry out a mechanical analysis of the rotor and design the nonmagnetic bandage (carbon fiber) covering the PM material.

Due to high-frequency currents, winding AC power losses are a crucial aspect of machine design. These losses include skin effect losses and proximity effect losses. Both effects were reduced by using litz wires, comprising multiple individually insulated conducting strands twisted or woven together.

All performance parameters of the studied machines were validated by 2D finite-element analysis (FEA) using the Simcenter Magnet software (Figure 14). Table 3 summarizes all the design parameters.

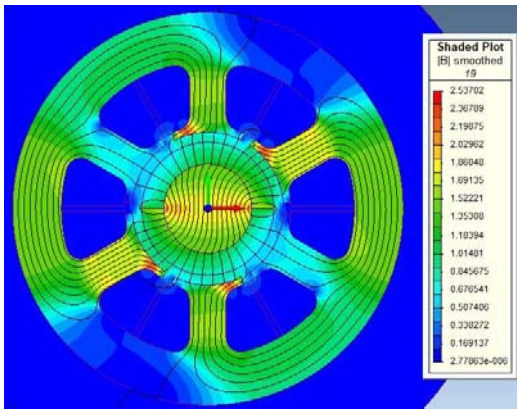

Figure 13. Flux density at rated torque.

Table 3. Design parameters of the high speed electric generator

Geometrical Data		Simulation Results	
Outer stator diameter	80 mm	Speed	160000 rpm
Outer rotor diameter	27 mm	Power	20 kW
Air gap	2 mm	Torque	1.25 Nm
Active length	25 mm	Efficiency	0.96
Stator slots	6		
Electrical data			
Number of phases	3		
Winding layout	double		
Conductor type	Litz wire		
Magnets	NdFeBr		
Magnet layout	Surface PM		

Finally, a prototype of the designed machine was built. The prototype generator components are shown in figure 15, showing the stainless-steel frame and the stator pack with the coils wound around the six teeth (a) and the PM rotor with the carbon fiber bandage (b). The 2-pole magnet is a single ring made of sintered Nd-Fe-B diametrically magnetized. High-speed hybrid ceramic ball bearings were selected for their simplicity and cost effectiveness.

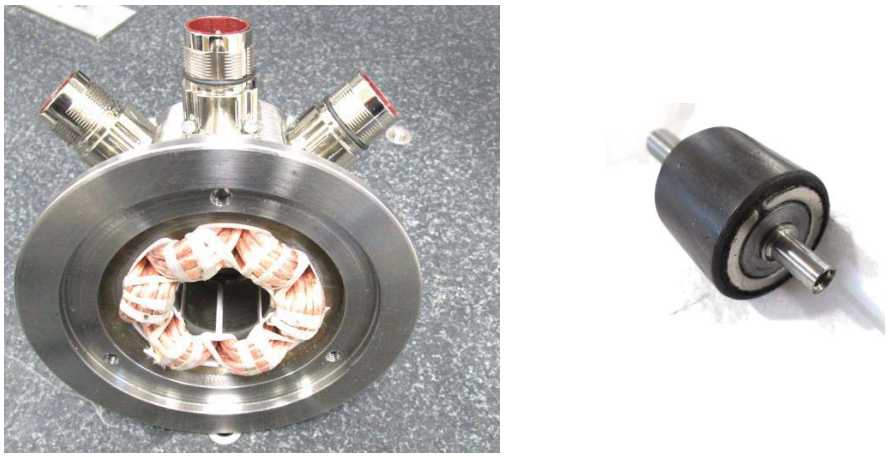

(a) (b)

Figure 14. HSM components. (a) Stator. (b) Rotor.

In order to estimate the winding characteristics and the air gap induction value, no-load fem were measured by driving the generator with a prime mover. The test is limited to a speed of 6000 rpm. (Fig. 14). By extrapolation, given the linearity between speed and no-load fem, the performance of the motor at rated speed can be derived. The value found agrees with the dimensioning value.

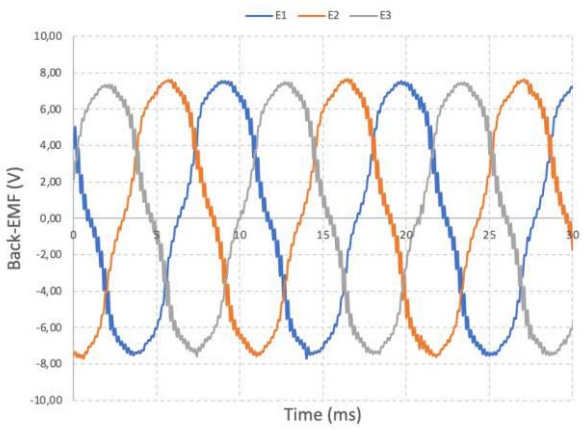

Figure 15. Back-EMF measuring @ 6000 rpm.

4 Conclusions

The present work shows the first result of a research aimed at verifying the betterments that can be obtained replacing the wastegate valve with a power turbine. On average, the power dissipated through the waste-gate valve in turbocharging applications is all but negligible since it can sum up to 17-18% of the engine's net power.

The considered study case analyses the behaviour of a 12.4L, 6 in-line cylinders, turbo charged diesel engine for marine, railway and truck applications. The analysis deals with the use of an auxiliary turbine to recover this dissipated work, added in parallel to the original turbocharger's turbine. The waste gate valve of the turbocharger, however, is left in place to

ensure that no extra supercharging pressure was achieved. Flow rate through the recovery turbine is controlled via a proper valve.

The engine fuel specific consumption decreases by 4.9% at maximum engine efficiency and by 7.7% at the maximum power condition. Besides this, the specific consumption curve is flatter. The engine achieves the best overall performance improvement with a recovery turbine sized to accommodate a flow rate between the flow available at the maximum torque and the maximum power regimes.

The problem of converting the mechanical work at the recovery turbine shaft can be solved by using high-speed/frequency electrical machines, equipped with permanent magnet, such as the one presented along this work, which proved to be compact and lightweight. The preliminary design process pointed out that this kind of machines can attain a very high conversion efficiency.

References

1. P. Fernández-Yáñez, O. Armas, R. Kiwan, A.G. Stefanopoulou, A.L. Boehman, A thermoelectric generator in exhaust systems of spark-ignition and compression-ignition engines. A comparison with an electric turbo-generator, Appl. Energy. 229 (2018) 80–87. https://doi.org/10.1016/j.apenergy.2018.07.107.
2. A. Kumar, D. Rakshit, A critical review on waste heat recovery utilization with special focus on Organic Rankine Cycle applications, Clean. Eng. Technol. 5 (2021) 100292. https://doi.org/10.1016/j.clet.2021.100292.
3. S. Broekaert, T. Grigoratos, D. Savvidis, G. Fontaras, Assessment of waste heat recovery for heavy-duty vehicles during on-road operation, Appl. Therm. Eng. 191 (2021) 116891. https://doi.org/10.1016/j.applthermaleng.2021.116891.
4. L. Shi, G. Shu, H. Tian, S. Deng, A review of modified Organic Rankine cycles (ORCs) for internal combustion engine waste heat recovery (ICE-WHR), Renew. Sustain. Energy Rev. 92 (2018) 95–110. https://doi.org/10.1016/j.rser.2018.04.023.
5. O. Farhat, J. Faraj, F. Hachem, C. Castelain, M. Khaled, A recent review on waste heat recovery methodologies and applications: Comprehensive review, critical analysis and potential recommendations, Clean. Eng. Technol. 6 (2022) 100387. https://doi.org/10.1016/j.clet.2021.100387.
6. R. Zhao, W. Zhuge, Y. Zhang, M. Yang, R. Martinez-Botas, Y. Yin, Study of two-stage turbine characteristic and its influence on turbo-compound engine performance, Energy Convers. Manag. 95 (2015) 414–423. https://doi.org/10.1016/j.enconman.2015.01.079.
7. H. Aghaali, H.E. Ångström, A review of turbocompounding as a waste heat recovery system for internal combustion engines, Renew. Sustain. Energy Rev. 49 (2015) 813–824. https://doi.org/10.1016/j.rser.2015.04.144.
8. J. Fu, J. Liu, Y. Wang, B. Deng, Y. Yang, R. Feng, J. Yang, A comparative study on various turbocharging approaches based on IC engine exhaust gas energy recovery, Appl. Energy. 113 (2014) 248–257. https://doi.org/10.1016/j.apenergy.2013.07.023.
9. U. Hopmann, M.C. Algrain, Diesel engine electric turbo compound technology, SAE Tech. Pap. (2003). https://doi.org/10.4271/2003-01-2294.
10. A.M.I. Bin Mamat, R.F. Martinez-Botas, S. Rajoo, A. Romagnoli, S. Petrovic, Waste heat recovery using a novel high performance low pressure turbine for electric turbocompounding in downsized gasoline engines: Experimental and computational analysis, Energy. 90 (2015) 218–234. https://doi.org/10.1016/j.energy.2015.06.010.

11. I. Arsie, A. Cricchio, C. Pianese, V. Ricciardi, M. De Cesare, Evaluation of CO2 reduction in SI engines with Electric Turbo-Compound by dynamic powertrain modelling, IFAC-PapersOnLine. 28 (2015) 93–100. https://doi.org/10.1016/j.ifacol.2015.10.014.
12. Pasini G., Frigo S., Antonelli M., Electric turbo compounding applied to a CI engine: A numerical evaluation of different layouts (2016) ASME 2016 Internal Combustion Engine Fall Technical Conference, ICEF 2016
13. I. Arsie, A. Cricchio, C. Pianese, V. Ricciardi, M. De Cesare, Modeling analysis of waste heat recovery via thermo-electric generator and electric turbo-compound for CO2 reduction in automotive SI engines, Energy Procedia. 82 (2015) 81–88. https://doi.org/10.1016/j.egypro.2015.11.886.
14. Y.H. Weilin Zhuge, Lei Huang, Wei Wei, Yangjun Zhang, Optimization of an Electric Turbo Compounding System for Gasoline Engine Exhaust Energy Recovery, (n.d.).
15. M. Algrain, Controlling an electric turbo compound system for exhaust gas energy recovery in a diesel engine, 2005 IEEE Int. Conf. Electro Inf. Technol. 2005 (2005). https://doi.org/10.1109/eit.2005.1627004.
16. B.P. Frigo S, Pasini G, Marelli S, Lutzemberger G, Capobianco M, Numerical evaluation of an electric turbo compound for SI engines., (2014). http://dx.doi.org/10.4271/2014-32-%0A0013.
17. F. Eggimann, S. Frigo, G. Lutzemberger, G. Pasini, L. Marmorini, Numerical Analysis of Electrically Assisted Turbocharger Application on Hybrid Vehicle, (2021) SAE Technical Papers.
18. F. Chmela and G. Orthaber, "Rate of heat release prediction for direct injection Diesel engines based on purely mixing controlled combustion", (1999) SAE technical paper 1999-01-0186
19. F. Chmela, G. Orthaber and W. Schuster, "Die Vorausberechnung des Brennverlaufes von Dieselmotoren mit direkter Einspritzung auf Basis des Einspritzverlaufs", (1998) MTZ 59, 7/8
20. A. Tenconi, S. Vaschetto and A. Vigliani, "Electrical Machines for High-Speed Applications: Design Considerations and Tradeoffs," in IEEE Transactions on Industrial Electronics, vol. 61, no. 6, pp. 3022-3029, June 2014, doi: 10.1109/TIE.2013.2276769.